Propagation dependence of chirp in Gaussian pulses and beams due to angular dispersion

Derong Li,[1] Shaoqun Zeng,[1,*] Qingming Luo,[1] Pamela Bowlan,[2,*] Vikrant Chauhan,[2] and Rick Trebino[2]

[1]*Britton Chance Center for Biomedical Photonics, Wuhan National Laboratory for Optoelectronics, Huazhong University of Science & Technology, Wuhan, 430074, China*

[2]*Georgia Institute of Technology, School of Physics 837 State Street NW, Atlanta, Georgia 30332 USA*

**Corresponding author: sqzeng@mail.hust.edu.cn pambowlan@gatech.edu*

Received November 26, 2008; revised February 11, 2009; accepted February 12, 2009; posted February 24, 2009 (Doc. ID 104611); published March 19, 2009

The chirp acquired by a Gaussian ultrashort pulse due to angular dispersion, unlike that of plane waves, increases nonlinearly with propagation distance and eventually asymptotes to a constant. However, this interesting result has never been directly measured. In this Letter, we use two-dimensional spectral interferometry to measure the propagation dependence of the chirp for Gaussian ultrashort pulses and beams with angular dispersion. The measured chirp as a function of propagation distance agreed well with theory. This work verifies both an equation and a measurement technique that will be useful for predicting or determining the pulse's chirp in ultrafast optics experiments that contain angular dispersion. © 2009 Optical Society of America

OCIS codes: 320.0320, 050.1940, 320.7100.

The linear chirp (we will call it "chirp" for simplicity) that an ultrashort pulse can acquire from angular dispersion is particularly useful in ultrafast optics, because it can be negative or positive (if imaging is used) and therefore offers much-needed control over the pulse's temporal duration [1–3]. Angular dispersion has also been used for other applications, such as achromatic phase matching [4], pulse shaping [5], and temporal focusing [6]. For these applications it is important to understand how the pulse's chirp changes as it propagates. The plane-wave [1–3] and Gaussian beam [7–9] models are commonly used to calculate the pulse's spectral phase due to propagating in the presence angular dispersion (where the chirp $\varphi^{(2)}$ is 1/2 of the coefficient of the second-order term in the Taylor expansion of the spectral phase). However, recent calculations have shown that the propagation dependence of the chirp of Gaussian pulses/beams due to angular dispersion is significantly different from that of plane waves [10,11].

The chirp introduced by a four-pass prism pulse compressor (assuming perfect alignment) has been verified to be consistent with both the plane-wave and the Gaussian beam models (see for example [12]). Ultrashort pulses have also been measured in the presence of angular dispersion [3,10,11,13–15], but, to our knowledge, the propagation dependence of the chirp has not been directly measured. Measuring the chirp due to angular dispersion is difficult, because large amounts of angular dispersion significantly increase the spot size and pulse duration, which decreases the peak power. While techniques such as frequency-resolved optical gating and GRENOUILLE can be used for measuring pulses with spatiotemporal couplings [14,15], these techniques are nonlinear and do not work well when the peak power is low. In this Letter, we use a linear technique called two-dimensional spectral interferometry (2DSI) [16,17] to measure the chirp of a Gaussian beam/pulse as a function of propagation distance after a single prism.

For the plane-wave model, the chirp introduced to the pulse by an angular disperser can be easily calculated using geometrical-optical ray tracing [1–3],

$$\varphi_p^{(2)} = -k\beta^2 z. \tag{1}$$

To obtain a more exact result, a two-dimensional Gaussian beam model of the pulse [considering $E(y,\omega,z)$] should be used. In this approach the Kirchhoff–Fresnel integral is used to numerically propagate the complex field [7,8] so that the expression for chirp can be derived by looking at the second-order term in the spectral phase of the complex field as a function z [11],

$$\varphi_g^{(2)} = -\frac{d(d+\alpha^2 z)+z_R^2}{(d+\alpha^2 z)^2+z_R^2}k\beta^2 z. \tag{2}$$

In these equations, the subscripts p and g denote plane-wave and Gaussian-beam models, respectively, and $k=2\pi/\lambda$ is the wave number, λ is the wavelength of the laser pulse, $z_R=\pi w_0^2/\lambda$ is the Rayleigh range, w_0 is the beam-waist size, d is the distance between the beam waist and the angular disperser, and z is the propagation distance after the angular disperser of the center frequency. The parameters α and β are the angular magnification and angular dispersion introduced by the disperser [7,8].

The two expressions for chirp shown in Eqs. (1) and (2) are quite different from each other. While $\varphi_p^{(2)}$ always increases linearly with propagation distance, $\varphi_g^{(2)}$ increases less rapidly and eventually asymptotes, which causes $\varphi_g^{(2)}$ to always be less than $\varphi_p^{(2)}$ after the same propagation distance z (with the same β). This is due to the decaying nature of the angular dispersion in a divergent Gaussian beam due to diffraction [10,11]. Another striking difference in the two equations is that $\varphi_p^{(2)}$, unlike $\varphi_g^{(2)}$, depends only on the angular dispersion and the propagation distance z and is independent of the Gaussian beam parameters.

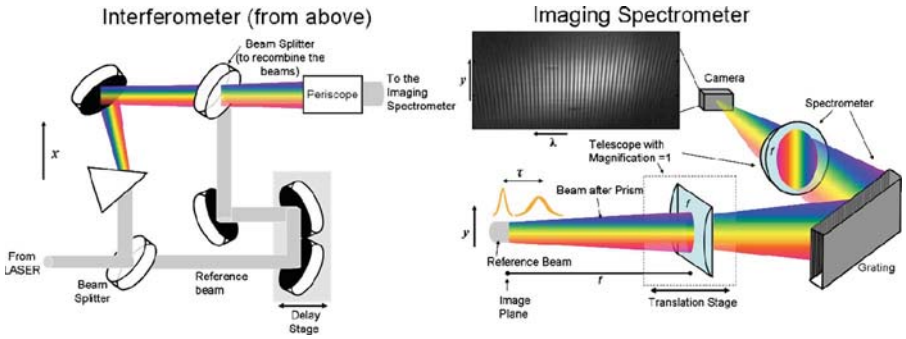

Fig. 1. (Color online) Schematic of the interferometer and the imaging spectrometer. (Left) The beam was spilt into a reference beam and an angularly dispersed beam, which were recombined with a second beam splitter, spatially flipped by 90° using a periscope, and then sent to the imaging spectrometer. The delay stage temporally separated the unknown and reference pulses by ~1 ps to yield spectral fringes. (Right) The imaging spectrometer used cylindrical and spherical lenses to image the vertical dimension onto the camera. The cylindrical lens was translated to vary the imaging plane so that the spectral phase of the angularly dispersed beam could be measured at different distances from the prism.

Also, unlike the Gaussian-beam model, the plane-wave model predicts that an increase in angular dispersion always introduces more chirp at a fixed value of z. These two different approaches only give different formulas when spatiotemporal couplings are present (in this case, angular dispersion), and when no couplings are present (i.e., a four-prism pass compressor), the chirp is equal to that given by the plane-wave model [7].

We performed an experiment to measure the propagation dependence of the chirp in Gaussian pulses/beams with angular dispersion. We used a KM Labs Ti:Sa oscillator and an SF14 prism to introduce angular dispersion. The detailed experimental parameters are: $\lambda_0 = 800$ nm, $\Delta\lambda = 20$ nm, $z_R = 0.19$ m, and $d = 2.0$ m. To measure the chirp as a function of propagation distance after the prism, we used a two-dimensional spectral interferometer [16,17], which includes mainly a Mach–Zehnder interferometer and an imaging spectrometer, as shown in Fig. 1. Note that in the presence of spatiotemporal couplings, the measured spectral phase depends on the orientation of the beam at the spectrometer; in our measurements y is the dimension in which the beam was angularly dispersed, and at every y we mapped wavelength onto the horizontal camera position, making the measured field the same one that we modeled.

To extract the spatiospectral phase $\varphi(y,\omega)$ from a single interferogram, we used a standard Fourier filtering method in which a one-dimensional Fourier transform of the data along the frequency axis isolated a phase-containing term from the spectra [18,19]. An inverse Fourier transform back to the frequency domain then yielded the spatiospectral phase introduced by the prism. We averaged the spatiospectral phase over y to obtain $\varphi(\omega)$ and then did a second-order curve fit to extract the chirp (or 1/2 of the coefficient of the $(\omega-\omega_0)^2$ term in the spatiospectral phase). Figure 2 shows a typical interferogram, the spectral phase retrieved from it, and a typical curve fit to the spectral phase.

To measure the pulse's chirp as a function of the propagation distance z, we translated the cylindrical lens in z, making the measurement at 18 locations from $z = 1.4$ to $z = 3.2$ m away from the prism in increments of 10 cm. Figure 3 shows the results of one measurement in which the beam entered the prism at Brewster's angle ($\gamma = 60.2°$), and the measured chirp as a function of z was compared to the theoretical curves using both the plane-wave and the Gaussian beam model.

This measurement agrees well with the calculation using the Gaussian beam model but is in strong disagreement with the results from the plane-wave model, which proves that the chirp calculated by the Gaussian beam model is more exact than that of the plane-wave model.

To verify how the chirp changes as we change the amount of angular dispersion introduced, we re-

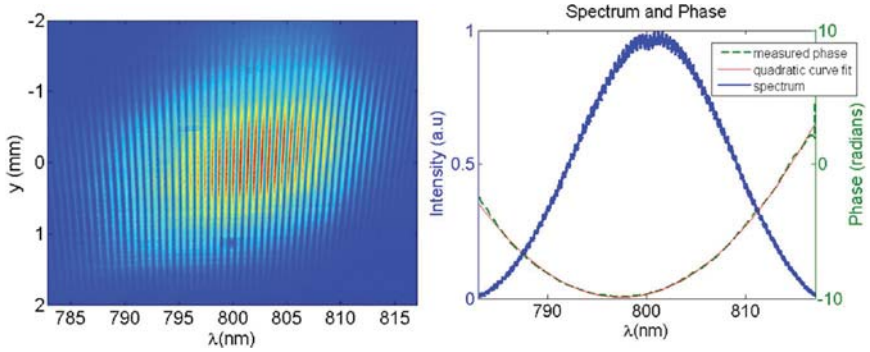

Fig. 2. (Color online) (Left) The 2DSI trace taken of the pulse 1.9 m after the prism. (Right) Retrieved spectrum and spectral phase from the interferogram at the left. The thin solid curve shows the curve fit used to extract the chirp.

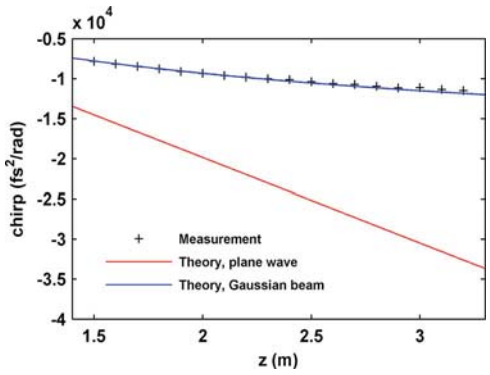

Fig. 3. (Color online) Chirp as a function of propagation distance z. The incidence angle is γ=60.2°.

peated this measurement at several other incidence angles, and these results are shown in Fig. 4. Again the measured chirp and the theoretical curves are in good agreement. As mentioned above, an increase in angular dispersion does not always introduce more chirp at a given propagation distance.

The minor discrepancy between the experiment and theory shown in Figs. 3 and 4 is likely due to several reasons. First, some positive chirp is introduced by the prism material, and this material thickness is difficult to accurately measure (the measured path length through the prism was used to add positive chirp to the theoretical curves shown in Figs. 3 and 4), so this could have been slightly off. Second, the difficulty in finely determining all of the experimental parameters (such as z_R, d, α, and β) also introduces some discrepancy. Finally, a small error could also have resulted due to the curve fitting to find the chirp from the spectral phase, although these curve fits were very close, as can be seen from Fig. 2, which shows a typical curve fit from our measurements (there was an rms error of 5 fs^2 in this fit, and all of others were similar to this). In our 2DSI setup we reconstruct the field with a spectral range of about 35 nm and a spectral resolution around 1 nm (accounting for the 10 times spectral resolution loss due to Fourier filtering [19,20]). This is enough spectral resolution for the measurements shown here, because the pulses were only from 40 to 800 fs long [13]. A detailed study of the error and resolution in spectral interferometry can be found in [20].

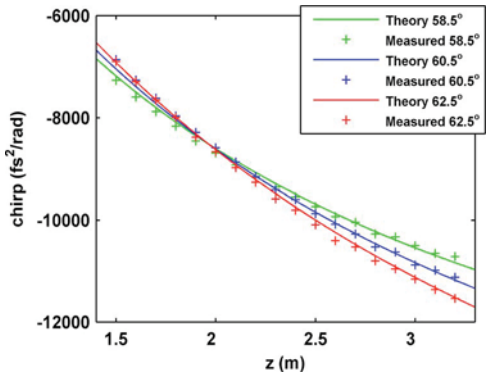

Fig. 4. (Color online) Chirp as a function of propagation distance z at different incident angles (γ=58.5°, 60.5°, 62.5°; a smaller incident angle provides larger angular dispersion). The theoretical curves use the Gaussian-beam model.

In summary, the evolution of the chirp of Gaussian ultrashort pulses/beams due to angular dispersion was experimentally verified using 2DSI. The chirp does not vary linearly with propagation distance as predicted by a plane-wave model. This result improves our understanding of how the chirp due to angular dispersion varies as the pulse propagates, and we illustrated a simple way to calculate or measure this chirp, which should be useful for applications of ultrafast optics where angular dispersion is involved.

This work was supported by the National Natural Science Foundation (NSFC) (60708025), 863 Project (2006AA020801), and Program for Changjiang Scholars and Innovative Research Team in University. R. T. and P. B. acknowledge support by National Science Foundation (NSF) Small Business Innovation Research grant 053-9595. P. B. also acknowledges support from the NSF fellowship IGERT-0221600.

References

1. S. Szatmari, G. Kuhnle, and P. Simon, Appl. Opt. **29**, 5372 (1990).
2. S. Szatmari, P. Simon, and M. Feuerhake, Opt. Lett. **21**, 1156 (1996).
3. K. Osvay, A. P. Kovacs, Z. Heiner, G. Kurdi, J. Klebniczki, and M. Csatari, IEEE J. Sel. Areas Commun. **10**, 213 (2004).
4. O. E. Martinez, IEEE J. Quantum Electron. **25**, 2464 (1989).
5. A. M. Weiner, J. P. Heritage, and E. M. Kirschner, J. Opt. Soc. Am. B **5**, 1563 (1988).
6. E. Tal, D. Oron, and Y. Silberberg, Opt. Lett. **30**, 1686 (2005).
7. O. E. Martinez, J. Opt. Soc. Am. B **3**, 929 (1986).
8. O. E. Martinez, Opt. Commun. **59**, 229 (1986).
9. Z. L. Horvath, Z. Benko, and A. Kovacs, Opt. Eng. (Bellingham) **32**, 2491 (1993).
10. K. Varjú, A. P. Kovács, K. Osvay, and G. Kurdi, Opt. Lett. **27**, 2034 (2002).
11. S. Zeng, D. Li, X. Lv, J. Liu, and Q. Luo, Opt. Lett. **32**, 1180 (2007).
12. S. Akturk, X. Gu, M. Kimmel, and R. Trebino, Opt. Express **14**, 10101 (2006).
13. P. Bowlan, P. Gabolde, M. A. Coughlan, R. Trebino, and R. J. Levis, J. Opt. Soc. Am. B **25**, A81 (2008).
14. S. Akturk, M. Kimmel, P. O'Shea, and R. Trebino, Opt. Express **11**, 491 (2003).
15. S. Akturk, M. Kimmel, P. O'Shea, and R. Trebino, Opt. Express **11**, 68 (2003).
16. J. Jasapara and W. Rudolph, Opt. Lett. **24**, 777 (1999).
17. W. Amir, T. A. Planchon, C. G. Durfee, J. A. Squier, P. Gabolde, R. Trebino, and M. Mueller, Opt. Lett. **31**, 2927 (2006).
18. L. Lepetit, G. Cheriaus, and M. Joffre, J. Nonlinear Opt. Phys. Mater. **5**, 465 (1996).
19. C. Froehly, A. Lacourt, and J. C. Vienot, Nouv. Rev. Opt. **4**, 183 (1973).
20. C. Dorrer, M. Joffre, L. Jean-Pierre, and N. Belabas, J. Opt. Soc. Am. B **17**, 1795 (2000).